



OPEN ACCESS

EDITED BY

Can Huang,
Pacific Gas and Electric Company, United States

REVIEWED BY

Siqi Bu,
Hong Kong Polytechnic University, Hong Kong SAR, China
Lu Zhang,
China Agricultural University, China
Hantao Cui,
North Carolina State University, United States

*CORRESPONDENCE

Zhao Xin,
✉ xinzhao@seu.edu.cn

RECEIVED 24 October 2024

ACCEPTED 15 January 2025

PUBLISHED 14 February 2025

CITATION

Xiaochen G, Haoran X, Xin Z, Shan G, Haixiang X, Ningyu Z, Qun L and Yue Y (2025) Dispatching of distribution networks with high permeability distributed new energy based on phase shifting transformer loop-closing device. *Front. Energy Res.* 13:1516459. doi: 10.3389/fenrg.2025.1516459

COPYRIGHT

© 2025 Xiaochen, Haoran, Xin, Shan, Haixiang, Ningyu, Qun and Yue. This is an open-access article distributed under the terms of the [Creative Commons Attribution License \(CC BY\)](https://creativecommons.org/licenses/by/4.0/). The use, distribution or reproduction in other forums is permitted, provided the original author(s) and the copyright owner(s) are credited and that the original publication in this journal is cited, in accordance with accepted academic practice. No use, distribution or reproduction is permitted which does not comply with these terms.

Dispatching of distribution networks with high permeability distributed new energy based on phase shifting transformer loop-closing device

Gao Xiaochen¹, Xu Haoran¹, Zhao Xin^{1*}, Gao Shan¹, Xie Haixiang¹, Zhang Ningyu², Li Qun² and Yang Yue¹

¹School of Electrical Engineering, Southeast University, Nanjing, China, ²State Grid Jiangsu Electric Power Co., Ltd. Research Institute, Nanjing, China

To address the issue of curtailment in wind and photovoltaic power due to high penetration of distributed renewable energy sources in multi-partition distribution networks, and to enhance operational efficiency and voltage quality, a day-ahead and intra-day scheduling strategy based on Phase Shifting Transformer (PST) loop-closing device is proposed. The day-ahead scheduling model aims to maximize the benefits from loop-closing operations by incorporating errors from new energy and load forecasts. Robust optimization techniques are employed to solve this model, resulting in the determination of the optimal loop-closing line. For intra-day scheduling, the focus is on minimizing the weighted sum of curtailment rate, voltage deviation rate, and network loss, thereby optimizing reactive power distribution and ensuring full utilization of renewable energy. Second-order cone programming is applied to the objectives and constraints to ensure convergence and expedite the solution process. Simulation results on an improved IEEE 33 bus test system demonstrate that the proposed day-ahead and intra-day scheduling strategy effectively leverages the voltage regulation and power flow control capabilities of PST loop-closing devices. This approach not only ensures the safety of the distribution network but also facilitates cross-regional integration of distributed renewable energy, reduces operational costs, and enhances overall network performance.

KEYWORDS

distributed new energy, high permeability, phase shifting transformer loop-closing device, distribution network, day-ahead and intra-day optimization, loop-closing operation

1 Introduction

With the increasing penetration of distributed renewable energy sources into distribution networks, the temporal mismatch between their output and load demand has intensified, exacerbating the “duck curve” phenomenon (Yang, 2022). This leads to situations where periods of high renewable energy output can cause reverse flows of net load, potentially resulting in line overloads, voltage limit violations, and subsequent curtailment of solar and wind energy (Xu B. et al., 2023; Hu et al., 2020). Consequently, effectively managing the integration of high-penetration distributed

renewable energy sources (DRES) through day-ahead and intra-day scheduling has become critical.

Current approaches to enhance the absorption of renewable energy in distribution networks include: utilizing market mechanisms to encourage proactive user responses to fluctuations in renewable energy output (Samadi et al., 2014), integrating energy storage systems and developing interactive strategies that encompass generation, network, load, and storage (Shen et al., 2015), and modifying line structures to resolve congestion (Li et al., 2018). Additionally, to address the uncertainty associated with distributed renewable energy sources, a day-ahead robust optimization model has been proposed to minimize operational costs (Li et al., 2024). Literature (Cong et al., 2019) proposes a two-stage coordinated control for distribution networks, optimizing network losses and absorption rates through network reconfiguration day-ahead and mitigating the impact of renewable energy randomness intra-day. Furthermore, the literature (Wang and Liu, 2022) incorporates the variability of electric vehicles, establishing a day-ahead and intra-day scheduling model that enhances renewable energy absorption while optimizing economic benefits for electric vehicle charging stations.

Previous studies predominantly address single distribution network partitions. However, actual distribution network is comprised of multiple partitions through interconnection lines. When one partition experiences curtailment of solar or wind power, resources from other partitions can be utilized, enabling cross-zone absorption of distributed new energy through loop-closing operation. Literatures (Gan et al., 2015; Wu et al., 2013) discuss the advantages of loop-closing operation, which allows unified management and scheduling of power resources across different partitions, thereby improving overall operational economy and reliability. Fault location and protection control within the context of loop-closing operation have been explored in the literature (Xue, 2020; Huang et al., 2019), ensuring that reliable performance of the whole distribution network is maintained.

Recent studies have explored loop-closing operations utilizing Soft Open Points (SOP). Curtailment penalties for wind and solar energy in day-ahead optimization objectives are introduced in the literature (Wang et al., 2024), with SOP being used to enhance active power transmission and reactive power compensation, thereby improving voltage distribution and facilitating distributed photovoltaic integration. Literature (Zheng and Shi, 2019) demonstrates that SOP-based loop-closing operation can rapidly respond to new energy fluctuations and achieve precise power flow control, effectively addressing low voltage issues under heavy loads and high voltage problems within renewable energy integration. Thus, closed loop operation for distributed new energy absorption shows feasibility and advantages; however, the high cost of numerous power electronic devices in SOP structures remains a challenge (Xu et al., 2024). Consequently, there is a need to investigate more cost-effective and technologically advanced loop-closing devices.

Phase Shifting Transformer (PST) loop-closing device can effectively compensate for the voltage phase angle difference across both sides of a line, reduce inrush currents during loop closing, and control line flow (Li et al., 2021; Xu et al., 2022). Literature (Yang et al., 2022) proposes an improved structure based on PST, highlighting its efficacy in addressing voltage imbalances across the line. Literature (Xu Z. et al., 2023) outlines the advantages of PST loop-closing device, noting its flexibility in controlling line flow, ease of operation and

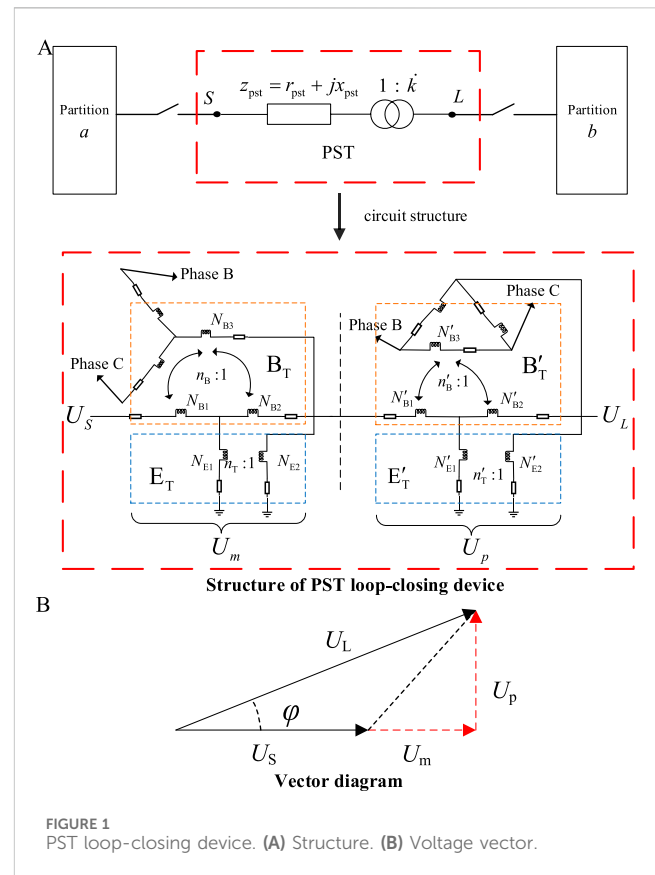


FIGURE 1
PST loop-closing device. (A) Structure. (B) Voltage vector.

maintenance, and significant economic benefits. Hence, PST loop-closing device has promising application prospects, and optimizing its day-ahead and intra-day scheduling strategies can substantially enhance the integration of DRES (Li et al., 2024).

In summary, this paper proposes a day-ahead and intra-day optimization scheduling strategy for distribution network with high permeability new energy based on PST loop-closing device. Initially, a mathematical model is developed based on the structure of PST loop-closing device. Subsequently, a comprehensive optimization scheduling model is proposed: in the day-ahead stage, robust optimization is employed to determine loop-closing line and corresponding periods; while in the intra-day stage, loop-closing periods and PST settings are adjusted to optimize the reactive power distribution. The model is then relaxed to second-order cone programming to accelerate the solution process. Finally, the effectiveness of the proposed strategy is validated using an improved IEEE 33 bus distribution network.

2 Phase shifting transformer loop-closing device model

As shown in Figure 1A, the PST loop-closing device is installed on the interconnection line between different distribution network partitions and is controlled by switches. S and L denote the two ends of the PST. This device can be modeled as an equivalent impedance z_{pst} in series with an ideal transformer with a complex ratio $k = ke^{j\varphi}$, where r_{pst} and x_{pst} are the equivalent resistance and reactance of the PST, respectively. k is the voltage magnitude adjustment ratio, and φ is the phase angle adjustment value. E_T and B_T represent the shunt

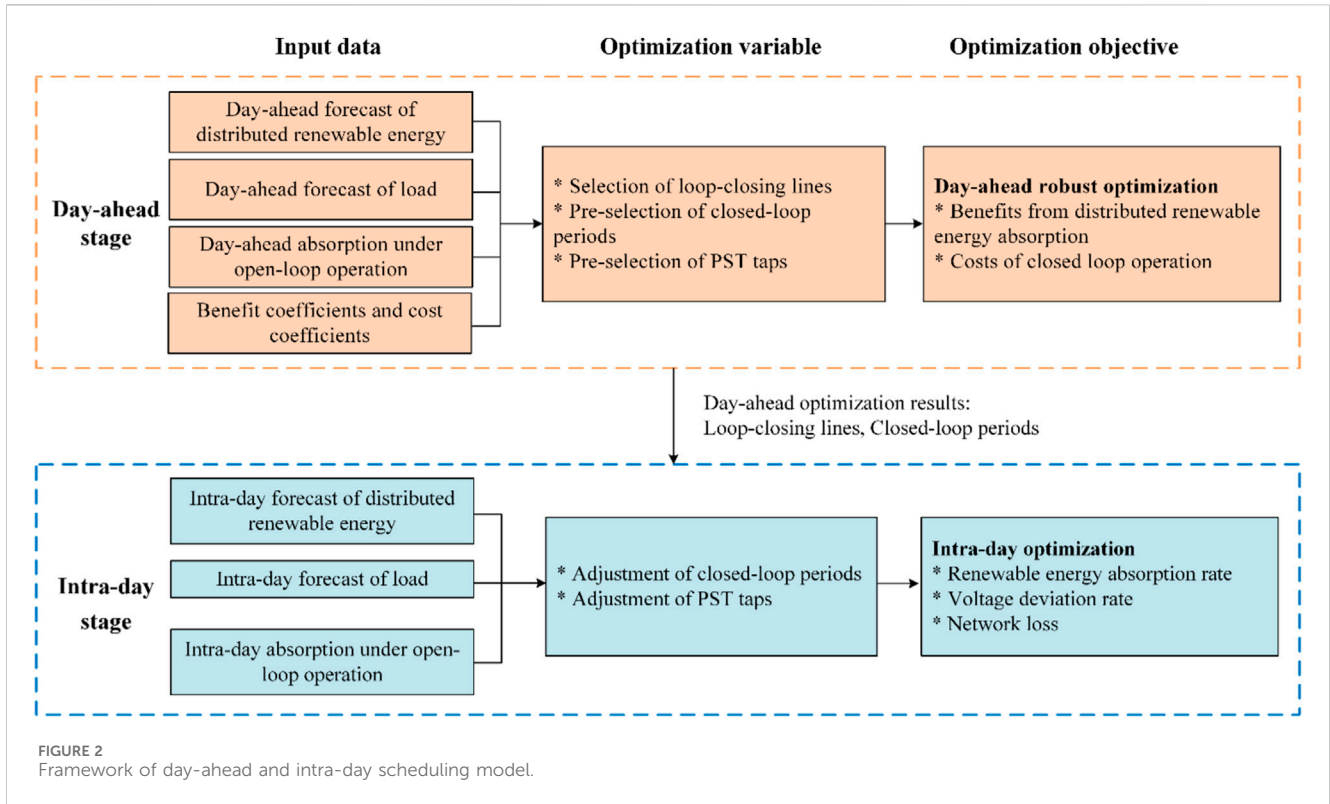


FIGURE 2 Framework of day-ahead and intra-day scheduling model.

and series transformers for adjusting the voltage magnitude, with their corresponding turn ratios n_T and n_B . The turns of the primary and secondary windings for E_T are denoted by N_{E1} and N_{E2} , respectively, while N_{B1} , N_{B2} and N_{B3} are the turns of windings 1, 2, and 3 of B_T . E'_T and B'_T denote the shunt transformer and series transformers for phase adjustment, with their corresponding turn ratios n'_T and n'_B . The turns of the primary and secondary windings of E'_T are represented by N'_{E1} and N'_{E2} , while N'_{B1} , N'_{B2} and N'_{B3} are the turns of windings 1, 2, and 3 of B'_T . These two parts are connected in series to achieve both the amplitude and phase control.

Figure 1B illustrates the voltage vector relationship for the PST. U_S and U_L denote the voltages at the start and end of the line, respectively, while U_M and U_P are used for magnitude and phase adjustment, respectively. From these relationships, the mathematical model can be derived as follows:

$$k = \frac{U_S}{U_L} = \frac{\frac{N_{B3}N_{E1}}{N_{B2}N_{E2}} - T_P}{\frac{N_{B3}N_{E1}}{N_{B2}N_{E2}} + T_P}$$

$$\varphi = 2 \arctan\left(\frac{\sqrt{3} N'_{B2}N'_{E2}}{N'_{B3}N'_{E1}} \times T_\varphi\right)$$

where T_P denotes the voltage magnitude adjustment setting, and T_φ represents the voltage phase adjustment setting.

3 Day-ahead and intra-day optimization scheduling based on PST loop-closing devices

This dissertation examines distribution networks characterized by high penetration of renewable energy sources. Given that distribution

networks are divided into multiple partitions, variations in renewable energy generation and load profiles across these regions are prevalent. Consequently, there may be instances where certain partitions experience surplus renewable energy generation, resulting in curtailment, while others with high demand could still accommodate additional renewable energy. In such scenarios, employing loop-closing operation in distribution network becomes a cost-effective scheduling strategy. Accordingly, this paper proposes a day-ahead and intra-day optimization scheduling strategy based on PST loop-closing devices to facilitate the cross-partition absorption of distributed renewable energy. The operational framework is illustrated in Figure 2.

In the day-ahead stage, closed loop lines are determined based on 24-h forecast results, with a focus on optimizing the economic efficiency from loop-closing operations while accounting for forecast errors. Corresponding closed-loop periods and PST settings are preliminarily selected. In the intra-day stage, the closed loop lines planned in the day-ahead stage are maintained. Rolling optimization is applied using updated forecast results to adjust the loop-closing time and PST settings, thereby optimizing the operational state of the distribution network while ensuring effective integration of renewable energy.

3.1 Day-ahead robust optimization model

3.1.1 Objective function

The day-ahead optimization is based on the 24-h forecast results with 1-h intervals, aiming to maximize the benefits from enhanced absorption and minimize the costs of closed loop operation of distribution networks. This process helps determine the lines that

need to be interconnected and identifies the corresponding time periods, thereby providing a reference for intra-day optimization. The objective function is expressed as follows:

$$\max f_{\text{profit}} = R_{\text{NE}} - C_{\text{LC}}$$

where f_{profit} denotes the benefits from closed-loop operation, R_{NE} represents the benefits from renewable energy absorption, and C_{LC} represents the closed-loop operational costs.

3.1.1.1 Benefits from renewable energy absorption

The increase in renewable energy absorption is quantified as the difference between the amount of renewable energy that can be absorbed under closed loop operation and in the initial open-loop state. The benefits from renewable energy absorption are derived from this increase.

$$R_{\text{NE}} = \sum_{t \in \Omega_T} \sum_{i \in \Omega_{\text{DG}}} r_{\text{DG}} \cdot (P_{\text{hh},i,t} - P_{\text{cs},i,t}) \cdot \Delta t$$

where Ω_T represents the set of all closed-loop periods; Ω_{DG} represents the set of all distributed renewable energy sources; Δt represents the length of each interval; r_{DG} represents the benefit coefficient for increased renewable energy absorption. $P_{\text{hh},i,t}$ is the power that can be absorbed by the distribution network under closed-loop operation from the i th renewable energy source during period t , while $P_{\text{cs},i,t}$ is pre-determined by solving the problem of maximizing renewable energy consumption under open-loop operation mode of distribution networks, in which the constraints are the same as in this optimization model. The key factors affecting the absorption include voltage limits, current overload, and reverse power flow constraints.

3.1.1.2 Costs of closed loop operation

The costs of closed loop operation primarily include switch operation costs, phase shifter adjustment costs, and the operational loss costs of PST during closed-loop periods.

$$C_{\text{LC}} = \sum_{t \in \Omega_T} \sum_{i \in \Omega_b} (c_{\text{switch}} \cdot |x_{\text{switch},i,t} - x_{\text{switch},i,t-1}| + c_{\text{tap}} \cdot x_{\text{tap},i,t} + c_{\text{loss}} \cdot x_{\text{switch},i,t} \cdot I_{\text{hh},i,t}^2 \cdot r_{\text{pst},i,t} \cdot \Delta t) \quad (1)$$

where Ω_b represents the set of all interconnection lines with PST; $x_{\text{switch},i,t}$ represents the switch status of the i th interconnection line during period t , where “1” indicates closed and “0” indicates open; $x_{\text{tap},i,t}$ represents the adjustment of the i th PST taps during period t , where “1” indicates a change in setting and “0” indicates no change. $I_{\text{hh},i,t}$ represents the current on the i th interconnection line during period t ; $r_{\text{pst},i,t}$ represents the equivalent resistance of the PST on the i th interconnection line. c_{switch} , c_{tap} , and c_{loss} are the cost coefficients for switch operation, PST adjustment, and PST operational losses, respectively.

3.1.2 Constraint

3.1.2.1 Distflow power flow constraint

$$\sum_{ij \in \Omega_l} (P_{ij,t} - r_{ij} \cdot I_{ij,t}^2) + P_{j,t} = \sum_{jk \in \Omega_l} P_{jk,t} \quad (2)$$

$$\sum_{ij \in \Omega_l} (Q_{ij,t} - x_{ij} \cdot I_{ij,t}^2) + Q_{j,t} = \sum_{jk \in \Omega_l} Q_{jk,t} \quad (3)$$

$$V_{i,t}^2 - V_{j,t}^2 = 2 \cdot (r_{ij} \cdot P_{ij,t} + x_{ij} \cdot Q_{ij,t} - (r_{ij}^2 + x_{ij}^2) \cdot I_{ij,t}^2) \quad (4)$$

$$I_{ij,t}^2 \cdot V_{j,t}^2 = P_{ij,t}^2 + Q_{ij,t}^2 \quad (5)$$

$$P_{j,t} = P_{j,t,\text{pv}} + P_{j,t,\text{wt}} - P_{j,t,\text{pst}} - P_{j,t,\text{load}} \quad (6)$$

$$Q_{j,t} = Q_{j,t,\text{pv}} + Q_{j,t,\text{wt}} - Q_{j,t,\text{pst}} - Q_{j,t,\text{load}} \quad (7)$$

where Ω_l represents the set of all branches; $P_{ij,t}$, $Q_{ij,t}$ and $I_{ij,t}$ represent the active power, reactive power and current from bus i to bus j at time t ; r_{ij} and x_{ij} represent the resistance and reactance of branch ij ; $P_{j,t}$ and $Q_{j,t}$ represent the active and reactive power injections at bus j at time t ; $V_{j,t}$ represent the voltage at bus j at time t ; $P_{j,t,\text{pst}}$ represents the active power of PST at bus j at time t ; $Q_{j,t,\text{pv}}$, $Q_{j,t,\text{wt}}$, $Q_{j,t,\text{pst}}$ and $Q_{j,t,\text{load}}$ represent the reactive powers of photovoltaic, wind power, PST and load at bus j at time t .

3.1.2.2 Safety constraints

The safety constraints primarily include voltage magnitude, branch current, renewable generation output and reverse power flow limits.

$$V_{\text{min}}^2 \leq V_{j,t}^2 \leq V_{\text{max}}^2 \quad (8)$$

$$I_{ij,t}^2 \leq I_{ij,\text{max}}^2 \quad (9)$$

$$P_{j,\text{pv},\text{min}} \leq P_{j,\text{pv}} \leq P_{j,\text{pv},\text{max}} \quad (10)$$

$$P_{j,\text{wt},\text{min}} \leq P_{j,\text{wt}} \leq P_{j,\text{wt},\text{max}} \quad (11)$$

$$P_{\text{ds},m} \leq P_{\text{ds},\text{max}} \quad (12)$$

where V_{max} and V_{min} represent the upper and lower limits of bus voltage; $I_{ij,\text{max}}$ represents the upper limit of I_{ij} ; $P_{j,\text{pv},\text{max}}$ and $P_{j,\text{pv},\text{min}}$ represent the upper and lower limits of photovoltaic output at bus j ; $P_{j,\text{wt},\text{max}}$ and $P_{j,\text{wt},\text{min}}$ represent the upper and lower limits of wind power output at bus j ; $P_{\text{ds},m}$ represents amount of reverse power flow in the m th partition; $P_{\text{ds},\text{max}}$ represents the upper limit of allowable reverse power flow for each partitions.

3.1.2.3 Loop-closing current constraint

$$I_{c,j} \leq I_{c,j,\text{max}} \quad (13)$$

where $I_{c,j}$ represents the loop-closing inrush current; $I_{c,j,\text{max}}$ represents the upper limit of the loop-closing inrush current.

3.1.2.4 PST settings constraint

$$\begin{aligned} T_{p,\text{min}} \leq T_p \leq T_{p,\text{max}}, T_p \in \mathbf{N} \\ T_{\varphi,\text{min}} \leq T_{\varphi} \leq T_{\varphi,\text{max}}, T_{\varphi} \in \mathbf{N} \end{aligned} \quad (14)$$

where $T_{p,\text{max}}$ and $T_{p,\text{min}}$ represent the upper and lower limits of the voltage magnitude adjustment settings; $T_{\varphi,\text{max}}$ and $T_{\varphi,\text{min}}$ represent the upper and lower limits of the phase angle adjustment settings. In this dissertation, the controllable PST settings range from -13 to $+13$.

3.1.2.5 Loop-closing operation frequency limit

$$\sum_{t \in \Omega_T} x_{\text{switch},i,t} \leq X_{\text{switch},i,\text{max}}$$

$$\sum_{t \in \Omega_T} \sum_{i \in \Omega_{\text{switch}}} x_{\text{switch},i,t} \leq X_{\text{switch,sum,max}}$$

where $X_{\text{switch},i,\text{max}}$ represents the maximum allowable number of loop-closing operations for interconnection line i within a day; $X_{\text{switch,sum,max}}$ represents the sum of the maximum allowable number of loop-closing operations for all lines within a day; Ω_{switch} represents the set of all interconnection lines.

3.1.3 Two-stage robust optimization model

Robust optimization addresses uncertainty factors by ensuring that the desired objective is achieved even under the worst-case scenarios within the uncertainty bounds. This paper employs a two-stage robust optimization approach that thoroughly considers uncertainties in renewable energy output and load forecasts.

The two-stage robust optimization model is formulated as follows:

$$\begin{aligned} & \max_x \left\{ \min_{\alpha \in \Omega_\alpha} \max_{y \in F(x,\alpha)} c^T y \right\} \\ & \text{s.t. } Dy \geq d \\ & \quad Ky = 0 \\ & \quad Fx + Gy \geq h \\ & \quad I_\alpha y = \alpha \end{aligned} \tag{15}$$

where x and y represent the decision variables of the first stage and the second stage, respectively; c represents the parameters corresponding to the decision variable y ; α represents the uncertainty variables; Ω_α represents the set of uncertainty variables; $F(x, \alpha)$ represents the feasible region of the second-stage decision variable y given x and α ; D, K, F, G and I_α are the constraint coefficient matrices; d and h are the constant vectors corresponding to the constraints.

For this paper, given the uncertainty in distributed renewable energy output and deviations in load forecast, the uncertainty set Ω_α for wind and solar output, as well as load forecasts, is defined as follows:

$$\Omega_\alpha = \left\{ \begin{array}{l} P_{pv}: \dot{P}_{j,t,pv} - \delta_{pv} \dot{P}_{j,t,pv} \leq \bar{P}_{j,t,pv} \leq \dot{P}_{j,t,pv} + \delta_{pv} \dot{P}_{j,t,pv} \\ P_{wt}: \dot{P}_{j,t,wt} - \delta_{wt} \dot{P}_{j,t,wt} \leq \bar{P}_{j,t,wt} \leq \dot{P}_{j,t,wt} + \delta_{wt} \dot{P}_{j,t,wt} \quad \forall j \in \Omega_u, \forall t \in \Omega_T \\ P_{load}: \dot{P}_{j,t,load} - \delta_{load} \dot{P}_{j,t,load} \leq \bar{P}_{j,t,load} \leq \dot{P}_{j,t,load} + \delta_{load} \dot{P}_{j,t,load} \end{array} \right\} \tag{16}$$

where $\bar{P}_{j,t,pv}$, $\bar{P}_{j,t,wt}$, $\bar{P}_{j,t,load}$ represent the uncertain forms of the photovoltaic, wind power, and load at bus j , respectively. $\dot{P}_{j,t,pv}$, $\dot{P}_{j,t,wt}$, $\dot{P}_{j,t,load}$ represent the forecast values of photovoltaic, wind power, and load, respectively. δ_{pv} , δ_{wt} , δ_{load} are the forecast error coefficients for photovoltaic, wind power, and load, respectively. Ω_u denotes the set of bus indices for all uncertain quantities.

The above model is structured into inner and outer layers. The outer layer addresses the first-stage problem, with the objective of maximizing the operational revenue from the distribution network closed loop operation. The first-stage decision variable x , encompasses the selection of the loop-closing lines and the PST taps. The inner min-max problem tackles the second-stage problem, aiming to identify the worst operational scenario. The second-stage decision variable y , primarily involves adjusting the settings of PST. The feasible region of y varies with different uncertain variables α and x .

To solve this two-stage robust optimization problem, it can be decomposed into a master problem and a sub-problem. By decomposing (Equation 15), the master problem is formulated as follows:

$$\begin{aligned} & \max_x z \\ & \text{s.t. } z \geq c^T y^l \\ & \quad Dy^l \geq d \\ & \quad Ky^l = 0 \\ & \quad Fx + Gy^l \geq h \\ & \quad I_\alpha y^l = \alpha^l \\ & \quad \forall l \leq k \end{aligned}$$

where l represents the current iteration number; k represents the total number of iterations; y^l , α^l represents the value of y , α after l iterations, respectively. The sub-problem can be represents as:

$$\min_{\alpha \in \Omega_\alpha} \max_{y \in F(x,\alpha)} c^T y$$

Using strong duality theory, this sub-problem is transformed into a maximization model for solution. Dual variables are introduced for various constraints as follows:

$$\begin{cases} Dy \geq d & \rightarrow \lambda \\ Ky = 0 & \rightarrow \gamma \\ Fx + Gy \geq h & \rightarrow \nu \\ I_\alpha y = \alpha & \rightarrow \pi \end{cases}$$

Where λ, γ, ν and π are the dual variables corresponding to each constraint. Consequently, the sub-problem can be transformed into the following form:

$$\begin{aligned} & \max_{u \in U^{\lambda,\gamma,\nu,\pi}} d^T \lambda + (h - Fx)^T \nu + \alpha^T \pi \\ & \text{s.t. } D^T \lambda + K^T \gamma + G^T \nu + I_\alpha^T \pi \leq c \\ & \quad \lambda \geq 0, \nu \geq 0, \pi \geq 0 \end{aligned}$$

Since the variables in the equation are bi-linear, the uncertainty variables, with their fluctuation ranges as given in (Equation 16), can also be expressed in the following form:

$$\alpha_i \pi_i = \alpha_{i,\text{min}} \pi_i + \eta_i \pi_i (\alpha_{i,\text{max}} - \alpha_{i,\text{min}})$$

where α_i denotes the i th uncertainty variable, $\alpha_{i,\text{max}}$ and $\alpha_{i,\text{min}}$ denote its upper and lower limits, respectively; π_i represents the dual variable of α_i , while η_i represents the auxiliary variable for α_i . This dissertation aims to determine the optimal solution under the worst-case scenario, taking into account the uncertainties in renewable energy and load output. The worst-case scenario typically arises at the extreme values of these fluctuations. Thus, η_i is set to either 0 or 1. The big M method is employed, which can be linearized into the following expression:

$$\begin{aligned} & \alpha_i \pi_i = \alpha_{i,\text{min}} \pi_i + \kappa_i (\alpha_{i,\text{max}} - \alpha_{i,\text{min}}) \\ & \quad -M \eta_i \leq \kappa_i \leq M \eta_i \\ & \quad -M(1 - \eta_i) + \pi_i \leq \kappa_i \leq M(1 - \eta_i) + \pi_i \end{aligned}$$

where κ_i represents a continuous auxiliary variable for α_i , and M is a large positive number.

3.1.4 Solution methodology

This dissertation employs the Columns and Constraints Generation (C&CG) algorithm for solving the problem. The

core principle of C&CG involves alternately generating columns and constraints, iteratively solving both the main problem and its sub-problems to progressively enhance solution quality until the optimal solution is obtain or predetermined termination conditions are met (Zeng and Zhao, 2013). Given that the objective of the day-ahead optimization is a max function, the main problem in the C&CG algorithm determines the upper bound of the objective, while the sub-problem updates the lower bound. The primary steps of the solution process are as follows:

- Step 1: Set the lower bound $LB = -\infty$ and upper bound $UB = +\infty$, initialize iteration count $k = 1$, randomly generate initial scenarios, and set convergence criterion ϵ .
- Step 2: Solve the primary problem, determine decision variables x^k and objective function value z^k , and update the upper bound $UB = \min \{UB, z^k\}$.
- Step 3: Substitute x^k into the sub-problem, determine the worst-case scenario u^k , decision variables y^k , and their corresponding objective function value $c^T y^k$, and update the lower bound $LB = \max \{LB, c^T y^k\}$.
- Step 4: Evaluate the convergence criterion $UB-LB \leq \epsilon$. If satisfied, terminate the loop and output scheduling results, decision variables, and objectives; otherwise, proceed to the next step.
- Step 5: Let $k = k + 1$, add cutting plane constraints $z \geq c^T y^{k-1}$, return to step 2, and repeat this process until the convergence condition is met.

3.2 Intra-day optimization model

The intra-day optimization is performed based on more accurate ultra-short-term forecasts and involves rolling optimization. While maintaining the loop-closing line determined by the day-ahead optimization, the intra-day optimization adjusts the PST taps to meet the loop-closing inrush current constraints, ensure the absorption rate of distributed renewable energy, and optimize system network losses and voltage deviation. The objective function can be represented as:

$$\begin{aligned} \min f &= \sigma_1 \cdot P_{qd} + \sigma_2 \cdot P_{loss} + \sigma_3 \cdot V_{py} \\ P_{qd} &= \sum_{t \in \Omega_T} \frac{P_{DG,t,sum} - \sum_{i \in \Omega_{DG}} P_{DG,i,t}}{P_{DG,t,sum}} \\ P_{loss} &= \sum_{t \in \Omega_T} \sum_{i \in \Omega_b} x_{switch,i,t} \cdot r_{i,t} \cdot \frac{P_{i,t}^2 + Q_{i,t}^2}{V_{i,t}^2} \cdot \Delta t \\ V_{py} &= \sum_{i \in \Omega_T} \sum_{i \in \Omega_n} \frac{|V_N - V_{i,t}|}{|V_N|} \end{aligned} \tag{17}$$

Where P_{qd} represents the curtailment rate of distributed renewable energy; P_{loss} represents the network losses; V_{py} represents the voltage deviation rate; $P_{DG,t,sum}$ represents the total output of distributed renewable energy sources at time t ; $P_{DG,i,t}$ represents the absorbable amount of i th distributed renewable energy at time t ; $r_{i,t}$ represents the resistance of the i th interconnection line at time t ; $P_{i,t}$ represents the active power of the i th interconnection line at

time t ; $Q_{i,t}$ represents the reactive power the i th interconnection line at time t ; $V_{i,t}$ represents the voltage of bus on the right side of the i th interconnection line at time t ; V_N represents the rated voltage; σ_1 , σ_2 and σ_3 represent weighting coefficients. In this dissertation, they are set to 0.4, 0.3, and 0.3 respectively. These coefficients can be adjusted according to specific requirements in practical applications.

The constraints for intraday optimization include (Equations 2–14). Additionally, there is the intra-day closed-loop period correction constraint:

$$\Delta t_{rn} \leq \Delta t_{rn,max}$$

Where Δt_{rn} represents the adjustment amount for intra-day closed-loop period; $\Delta t_{rn,max}$ represents the maximum allowable adjustment amount for intra-day closed-loop period.

3.3 Second-order cone transformation of the model

The objective function and constraints in this paper involve numerous nonlinear models, which are non-convex and difficult to solve, often leading to local optima. This paper employs second-order cone optimization to reformulate these nonlinear models into linear equations, facilitating easier convergence of the objective function and accelerating the solution process while ensuring optimal results (Chowdhury et al., 2023; Liu et al., 2014). The revised model is equivalent to a mixed-integer linear programming problem, which can be directly solved using commercial solvers.

In the day-ahead optimization model, the objective function in Equation 1 is replaced with:

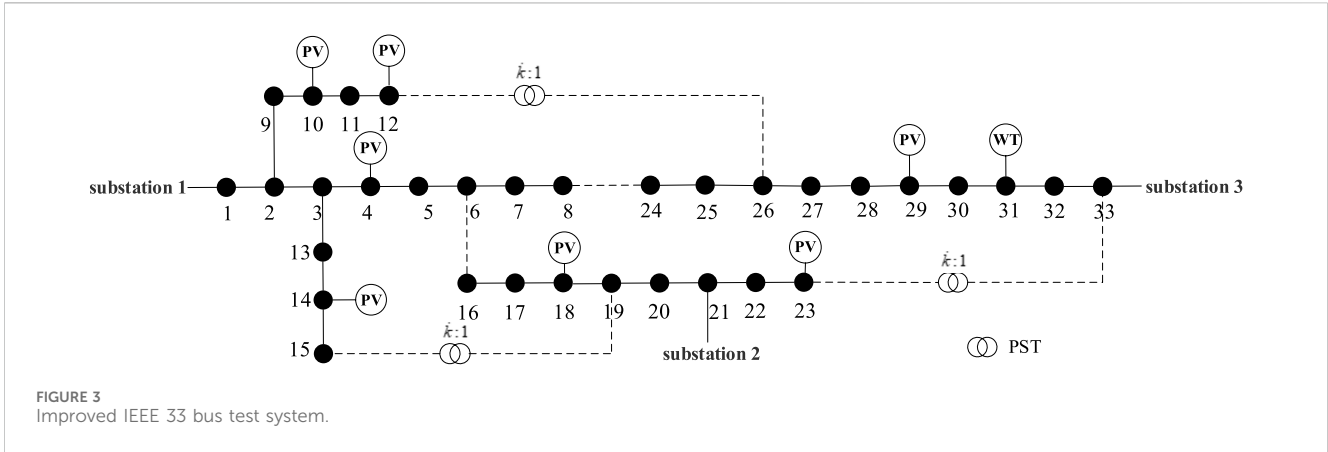
$$\begin{aligned} C_{LC} &= \sum_{t \in \Omega_T} \sum_{i \in \Omega_b} (c_{switch} \cdot |x_{switch,i,t} - x_{switch,i,t-1}| + c_{tap} \cdot x_{tap,i,t} \\ &\quad + c_{loss} \cdot x_{switch,i,t} \cdot I_{hl,i,t} r_{pst,i,t} \cdot \Delta t) \end{aligned}$$

By substituting the quadratic terms in the objective function (Equation 17) by replacing $V_{i,t}^2$ with $V_{i,t}^*$, it can be expressed as follow

$$P_{loss} = \sum_{t \in \Omega_T} \sum_{i \in \Omega_b} x_{switch,i,t} \cdot r_{i,t} \cdot \frac{P_{i,t}^2 + Q_{i,t}^2}{V_{i,t}^*} \cdot \Delta t$$

The constraints in Equations 2–5, 8, 9 are linearized by replacing $I_{ij,t}^2$, $V_{i,t}^2$ and $V_{j,t}^2$ with their respective second-order cone representations $I_{ij,t}^*$, $V_{i,t}^*$ and $V_{j,t}^*$. The resulting linearized expressions are:

$$\begin{aligned} \sum_{ij \in \Omega_l} (P_{ij,t} - r_{ij} \cdot I_{ij,t}^*) + P_{j,t} &= \sum_{jk \in \Omega_l} P_{jk,t} \\ \sum_{ij \in \Omega_l} (Q_{ij,t} - x_{ij} \cdot I_{ij,t}^*) + Q_{j,t} &= \sum_{jk \in \Omega_l} Q_{jk,t} \\ V_{i,t}^* - V_{j,t}^* &= 2 \cdot (r_{ij} \cdot P_{ij,t} + x_{ij} \cdot Q_{ij,t} - (r_{ij}^2 + x_{ij}^2) \cdot I_{ij,t}^*) \\ I_{ij,t}^* \cdot V_{j,t}^* &= P_{ij,t}^2 + Q_{ij,t}^2 \\ V_{min}^2 &\leq V_{j,t}^* \leq V_{max}^2 \\ I_{ij,t}^* &\leq I_{ij,max}^2 \end{aligned}$$



4 Case study

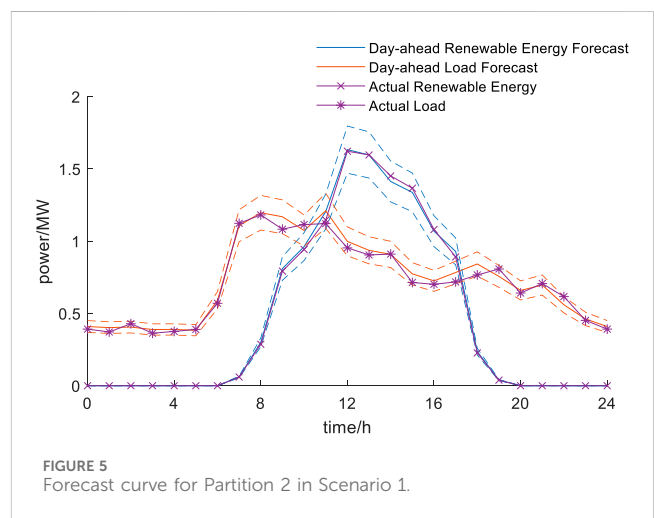
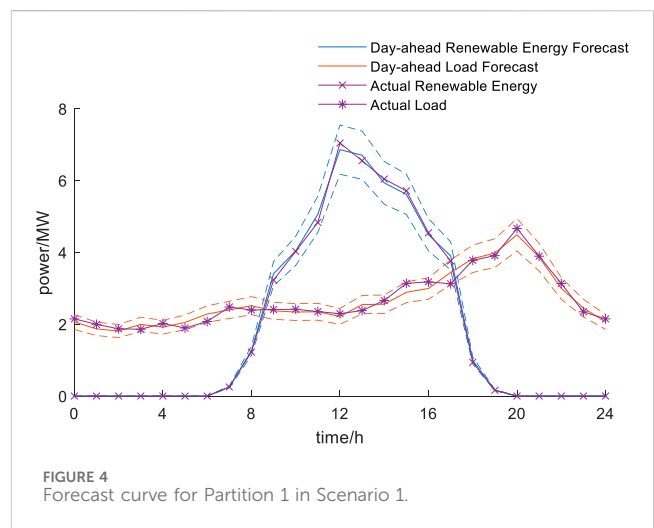
This paper adapts the IEEE 33 bus test system using data from a real distribution network, as shown in Figure 3. The network consists of three grid partitions (Bus 1-Bus 15, Bus 16-Bus 23, and Bus 24- Bus 33, designated as Partition 1–3, respectively). There are five interconnection lines between these partitions. Based on the characteristics of renewable energy and load, three of them include PST loop-closing devices, specifically Line 12–26, 15–19, and 23–33. Partition 1 and 2 are equipped with distributed photovoltaic generation, while Partition 3 contains one distributed PV and one dispersed wind turbine. The total penetration rate in the model reaches 97% based on installed capacity.

4.1 Analysis of day-ahead optimization result

To set up the day-ahead stage, the load forecast deviation to within $\pm 5\%$. The following three scenarios are selected for verification:

- Scenario 1: The proposed strategy is implemented, and the error between the day-ahead forecast and actual data for distributed renewable energy does not exceed 5%.
- Scenario 2: The proposed strategy is implemented, and the error between the day-ahead forecast and actual data for distributed renewable energy does not exceed 10%.
- Scenario 3: A deterministic method based on forecast data is applied, with the error between the day-ahead forecast and actual data for distributed renewable energy not exceeding 5%.

The day-ahead forecasts of renewable generation and load for each zone in Scenario 1 are shown in Figures 4–6. The different colored dashed lines represent the upper and lower limits of the fluctuation range for renewable energy and load. The load demand in each partition corresponds to the characteristics of the respective zone. It is evident that throughout the day, all three partitions experience renewable generation exceeding load. Notably, Partition 1 faces the most severe issue, with PV output exceeding load by 300% at 13:00. Further analysis reveals that since PV are primarily installed at the end of the feeders, accommodating all the renewable energy would lead to voltage violations at Bus 11 and 12. At the same



time, the end nodes in Partition 3 have heavier loads and lower distributed renewable output, indicating some remaining absorption capacity. This analysis highlights that due to the uneven distribution of renewable energy and load across the network partitions, issues

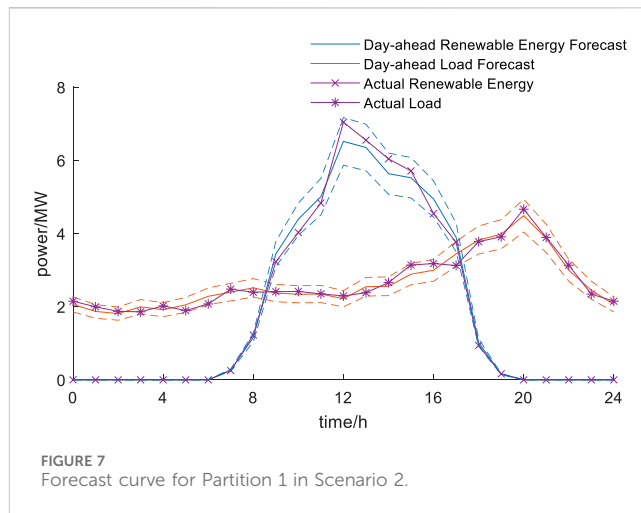
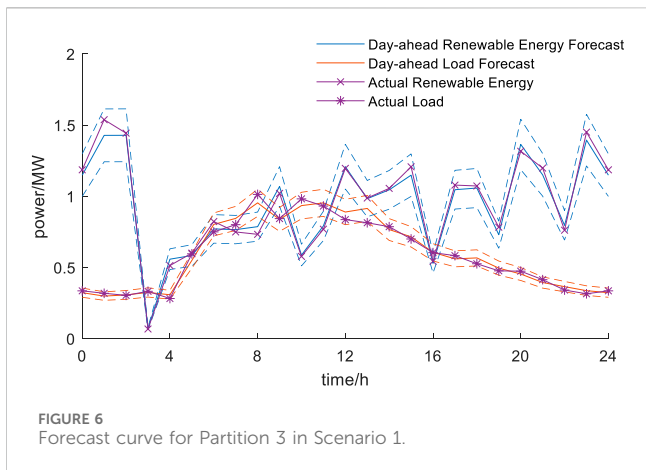


TABLE 1 Optimize parameter settings.

Parameter	Value	Parameter	Value
$r_{DG}/(\text{¥}/\text{kW})$	0.8	$\delta_{pv}/\%$	10
$c_{loss}/(\text{¥}/\text{kW})$	5	$\delta_{wt}/\%$	15
$c_{switch}/\text{¥}$	30	$\delta_{load}/\%$	5
$c_{tap}/\text{¥}$	20		

such as line current overloads, voltage violations, or curtailment of wind and solar energy may arise. Effective and reasonable loop-closing operation in the distribution network could potentially address these absorption challenges.

Given the varying renewable energy and load conditions across different periods, a day-ahead dispatch plan is formulated. The parameters for the day-ahead optimization refer to references (Li, 2019; Xiong et al., 2021), as shown in Table 1. The maximum reverse power flow for each partition is 6 MW. The time interval is set to 1 h. Each interconnection line can operate in a closed loop most once per day, with no limit on the duration of each loop-closing operation. The total number of loop-closing operations for all interconnection lines in a day is limited to a maximum of three. Within each time periods, the PST loop-closing device can be adjusted at most once. The optimization results using the proposed strategy are presented in in Table 2.

According to the proposed method, line 12–26 is selected for closed loop operation between 11:00 and 15:00, while the

connection of line 15–19 is selected for the period from 15:00 to 16:00. Overall, the approach achieves 100% utilization of distributed renewable energy output within a day. This outcome is attributed to the fact that the total benefits from interconnection lines are closely related to the increased renewable energy utilization. In contrast, the closed-loop operation costs remain relatively fixed. This is because the switching operation and phase shifter adjustment costs are generally fixed, while the operational loss costs of PST loop-closing device is primarily influenced by the interconnection line current. Since loop-closing current constraint is considered, the PST loop-closing device helps reduce this current. Moreover, by adequately accounting for the variability of wind and solar resources and load forecasting errors, the method ensures that the total revenue reaches 2,613.65 yuan even under the most adverse conditions.

The forecasts of renewable generation and load of Scenario 2 are illustrated in Figures 7–9. In this scene, a larger forecast error is observed for distributed renewable energy. Utilizing the two-stage robust optimization method outlined in this chapter, with parameters identical to those used in Scenario 2, the results are presented in Table 3.

After optimization in Scenario 2, distributed renewable energy can be fully accommodated. The optimized periods and lines for closed loop operation are identical to those in Scenario 1. However, the settings of PST differ from Scenario 1. Under Scenario 2 optimization, a profit of 2,326.29 yuan is achievable

TABLE 2 Scenario 1 day-ahead optimization results.

Closed-loop period	Loop-closing line	PST taps/ $[T_{\varphi}, T_P]$	Closed-loop benefit/¥	Total benefit/¥
11:00–12:00	12–26	[0,2]	140.31	2,613.65
12:00–13:00		[1,9]	921.52	
13:00–14:00		[1,7]	722.67	
14:00–15:00		[-2,1]	506.55	
15:00–16:00	15–19	[2,1]	322.60	

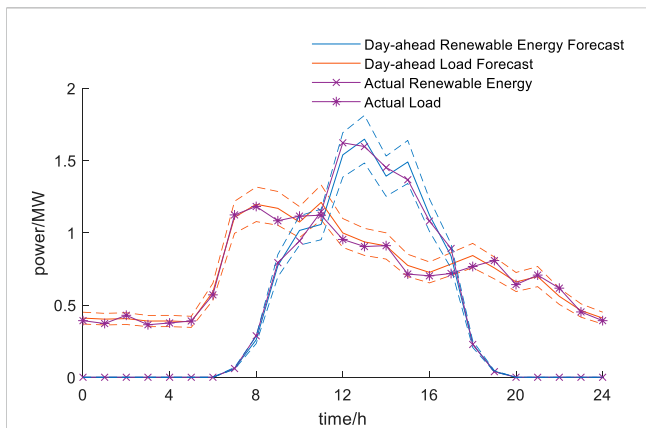


FIGURE 8 Forecast curve for Partition 2 in Scenario 2.

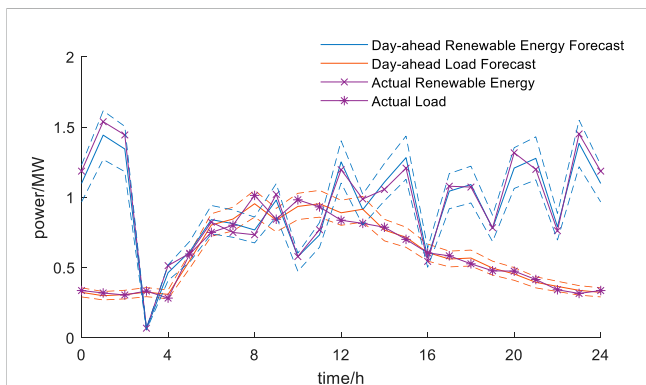


FIGURE 9 Forecast curve for Partition 3 in Scenario 2.

even under the worst-case scenario of fluctuating distributed renewable energy and loads. The profit during 11:00–15:00 is reduced compared to Scenario 1, due to Scenario 2’s prediction of less distributed renewable energy that the open-loop network cannot accommodate. Conversely, the profit during 15:00–16:00 increases compared to Scenario 1, as Scenario 2 predicts more distributed renewable energy that the open-loop network cannot accommodate. Overall, the total profit under robust optimization in Scenario 2 decreases by 287.36 yuan compared to Scenario 1.

Comparison between Scenario 2 and Scenario 1 indicates that the strategies proposed in this chapter demonstrate robust performance across varying prediction error ranges. The loop-closing lines and periods established in Scenario 1 are equally applicable in Scenario 2, with difference only in the taps of PST. This underscores the effectiveness and feasibility of the day-ahead optimization model developed.

In Scenario 3, by disregarding uncertainties and employing the optimization objectives and deterministic constraints as proposed in this paper based on forecast data, the day-ahead loop-closing scheduling is formulated. The distributed renewable energy and load data for each partition are based on the day-ahead forecast data from Scenario 1. The optimization results are detailed in Table 4.

According to the results in Table 3, utilizing forecast-based methods allows for loop-closing operation for line 12–26 during 11:00–16:00, achieving a total profit of 3,187.16 yuan. This profit is influenced by specific forecast scenarios. However, due to prediction errors, there are instances where the loop-closing operation of line 12–26 during 15:00–16:00 may fail to meet 100% integration requirements.

Additionally, from a strategic perspective, the day-ahead scheduling determines the specific closed loop periods and lines for the entire day, emphasizing a comprehensive and robust planning approach. In contrast, intra-day scheduling prioritizes precision in control. Consequently, the results obtained from the two-stage robust optimization method are better suited to the day-ahead optimization context, ensuring compliance within the bounds of prediction errors.

4.2 Analysis of intra-day optimization result

During the intra-day stage, optimization is conducted using more precise ultra-short-term load forecasts, without modifying the loop-closing lines determined in the day-ahead plan. To accommodate the integration of new energy and account for potential abnormal fluctuations in renewable generation, the timing of loop-closing is permitted to be adjusted by up to 1 h. In this study, the error between intra-day forecasts and actual data is kept within 3%, with no observed abnormal fluctuations in the intra-day forecasting results. The intra-day renewable energy and load forecast curves for each partition are shown in Figures 10–12.

During the intra-day stage, closed loop operation are scheduled at 11:00 and 15:00, with pre-determined settings for

TABLE 3 Scenario 2 day-ahead optimization results.

Closed-loop period	Loop-closing line	PST taps/[T_{φ}, T_P]	Closed-loop benefit/¥	Total benefit/¥
11:00–12:00	12–26	[−3,4]	65.26	2,326.29
12:00–13:00		[4,2]	844.92	
13:00–14:00		[1,3]	608.68	
14:00–15:00		[2,6]	387.85	
15:00–16:00	15–19	[−1,2]	419.58	

TABLE 4 Scenario 3 day-ahead optimization results.

Closed-loop period	Loop-closing line	PST taps/[T_φ, T_P]	Closed-loop benefit/¥	Total benefit/¥
11:00–12:00	12–26	[3,2]	265.93	3,187.16
12:00–13:00		[-1,6]	1016.52	
13:00–14:00		[-1,6]	910.96	
14:00–15:00		[3,2]	543.03	
15:00–16:00		[1,2]	450.72	

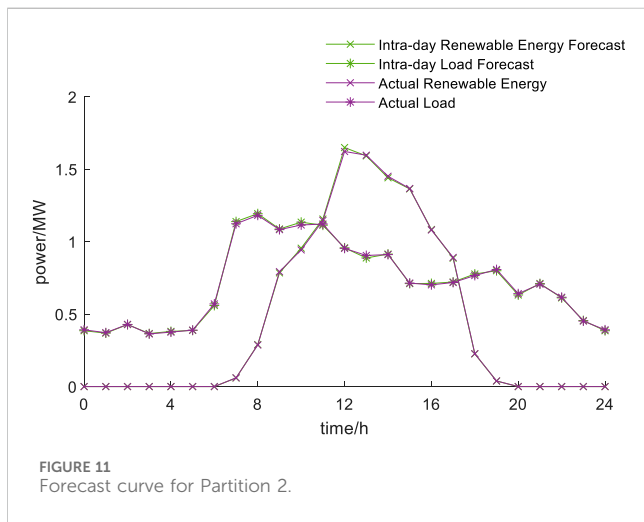
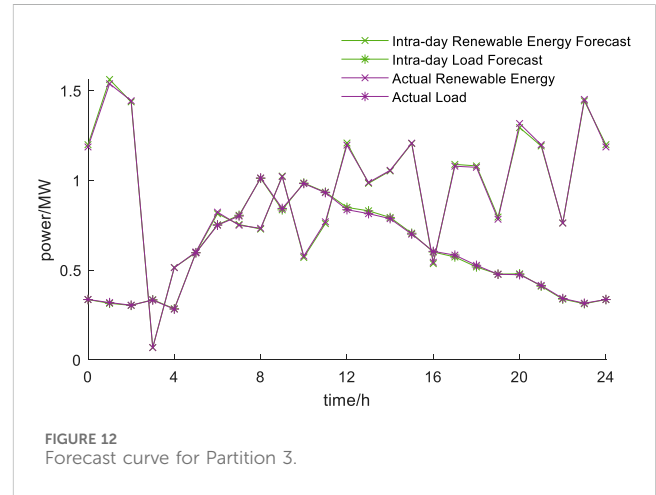
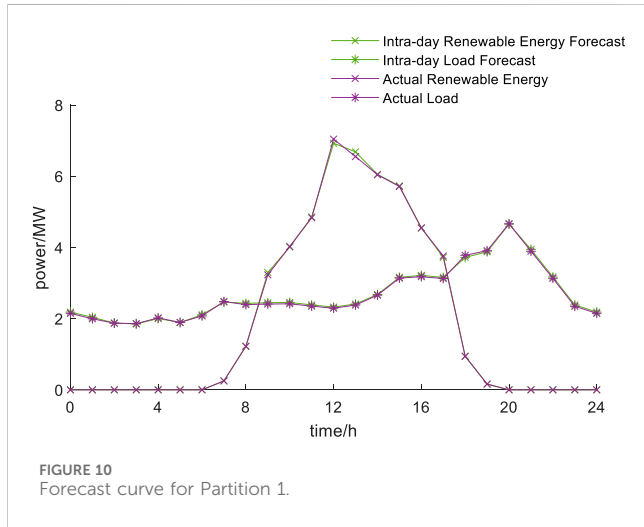


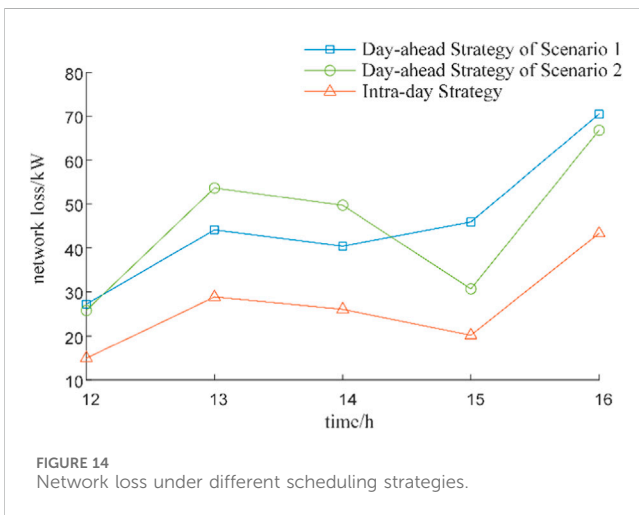
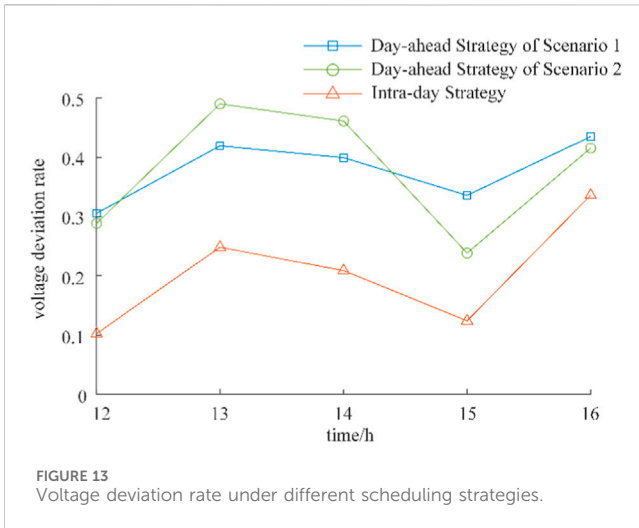
TABLE 5 Intra-day optimization results.

Period	Loop-closing line	PST taps/[T_φ, T_P]
11:00–12:00	12–26	[9,2]
12:00–13:00		[8,3]
13:00–14:00		[8,3]
14:00–15:00		[8,2]
15:00–16:00	15–19	[-3,0]

PST. At 11:00, the PST taps are [5,11], resulting in a loop-closing transient current of 31.76 A. At 15:00, the PST settings are [-7,4], yielding a loop-closing transient current of 25.14 A. These settings are designed to minimize the loop-closing transient currents. The results obtained from applying the intra-day optimization strategy proposed in this chapter are summarized in Table 5.

The intra-day optimization results maintain the closed loop lines and periods determined in the day-ahead plan. Under the intra-day plan, the renewable energy integration rate also reaches 100%. Compared to the day-ahead plan, adjustments to the settings of PST are made due to reactive power optimization, ensuring optimal network performance during each time period. Figures 13, 14 illustrate the voltage deviation rate and network losses, respectively, for the day-ahead strategies of Scenario 1 and 2 and intra-day scheduling plan, based on the intra-day forecast data.

From the figures, it is evident that with more accurate intra-day forecasts, the intra-day loop-closing scheduling plan achieves reduction in both voltage deviation and network losses compared to the day-ahead plan. The settings of PST provided under different day-ahead forecast accuracies result in varying



voltage deviations and network losses when applied to intra-day forecast data. However, with the unified adjustments made through intra-day optimization, the network can achieve optimal operating conditions. Therefore, the intra-day optimization strategy enhances the accuracy of PST settings, effectively mitigating the impact of day-ahead forecast errors. By maintaining the closed-loop lines constant, this approach ensures complete integration of distributed renewable energy, reduces overall voltage deviation and network losses, and improves voltage and power flow distribution.

4.3 Analysis of the effects of different loop-closing scheduling plan

To assess the effectiveness of various loop-closing scheduling plans under actual distributed renewable generation and load, three cases are set up:

Case 1: Implementation of the day-ahead scheduling plan based on forecast data.

Case 2: Application of the day-ahead scheduling plan derived from the two-stage robust optimization in Scenario 1.

Case 3: Utilization of the intra-day scheduling plan obtained through rolling optimization.

Based on the scheduling plans of these cases, the actual data was used for validation. The results are presented in Table 6.

In Case 1, line 12–26 remain in loop-closing operation from 15:00 to 16:00. However, under actual conditions, the renewable generation in Partition 3 during this period exceeds the day-ahead forecast, while the load is slightly reduced. This results in increased voltage near the interconnection line in Partition 3, thereby limiting the amount of renewable energy that can be accommodated. Consequently, the profit from loop-closing operation decreases significantly, with a reduction of 667.37 yuan compared to the projected total profit under the day-ahead forecast, as shown in Table 2. This demonstrates that the method used in Case 1 has notable limitations and not applicable under actual conditions.

A comparison between Case 2 and Case 1 indicates that the results from robust optimization in the day-ahead stage are more generalizable, achieving at least the expected profit within the forecast error range. The total profit of Case 3 is comparable to that of Case 2; however Case 3 features more precise adjustments of PST settings, leading to reduced operational loss costs and avoiding the expense of an additional adjustment. As a result, the total profit of Case 3 is higher. Additionally, Case 3 achieves a lower overall voltage deviation and network losses compared to Case 2, as depicted in Figures 15, 16, which aligns closely with the results under intraday forecasts. This demonstrates the comprehensiveness and effectiveness of the strategy proposed in this paper.

5 Additional requirements

This dissertation addresses the challenge of curtailing wind and solar energy in distribution network with high penetration of distributed renewable energy. It proposes a day-ahead and intra-day scheduling strategy utilizing PST loop-closing devices to achieve cross-partition renewable energy integration within the distribution network. This strategy employs robust optimization during the day-ahead stage to account for the randomness of renewable energy and load, selecting the loop-closing lines to ensure operational safety while developing an economically optimal day-ahead plan. During the intra-day stage, optimization is performed based on more accurate forecasts, adjusting closed-loop periods and PST settings to optimize voltage and power flow in the distribution network without altering the selected loop-closing lines.

The results demonstrate that the proposed day-ahead and intra-day scheduling strategy using PST loop-closing device significantly enhances the safe and economical operation of the distribution network. First, when certain partitions experience curtailment of wind and solar energy, the PST loop-closing device facilitates cross-partition integration, thereby improving the overall utilization rate and operational economy of the distribution network. Secondly, the power flow

TABLE 6 Optimization results for different cases.

Period	Case 1		Case 2		Case 3	
	Closed-loop benefit/¥	Total benefit/¥	Closed-loop benefit/¥	Total benefit/¥	Closed-loop benefit/¥	Total benefit/¥
11:00–12:00	210.63	2,519.79	214.18	2,880.83	214.59	2,903.34
12:00–13:00	920.24		919.83		920.15	
13:00–14:00	810.87		793.18		813.88	
14:00–15:00	517.07		517.72		518.09	
15:00–16:00	60.98		435.92		436.63	

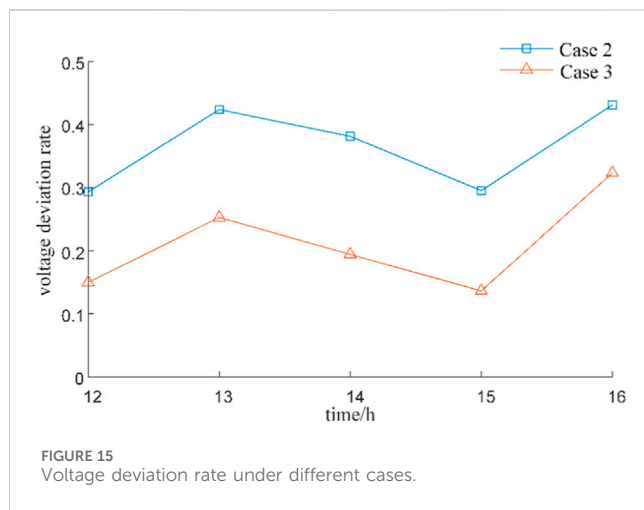


FIGURE 15 Voltage deviation rate under different cases.

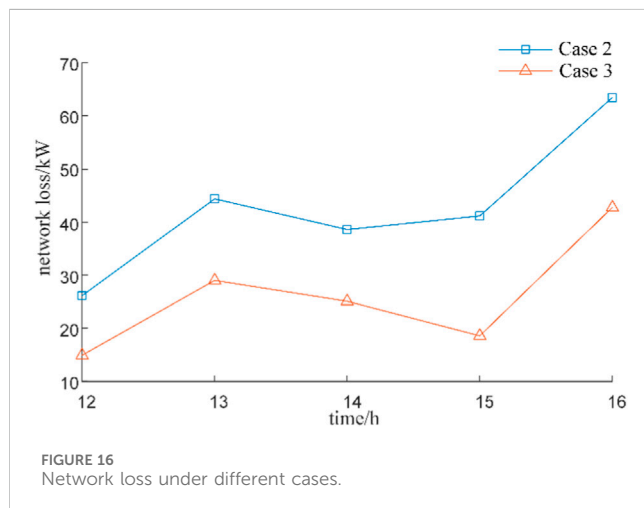


FIGURE 16 Network loss under different cases.

control capabilities of the PST effectively reduce voltage deviation and network losses, optimizing the operation state of the distribution network. Additionally, PST can reduce loop-closing currents, ensuring the safety of loop-closing operations. In summary, the strategy proposed in this dissertation shows promising prospects for addressing the integration challenges of high-penetration renewable energy in future distribution network.

Data availability statement

The raw data supporting the conclusions of this article will be made available by the authors, without undue reservation.

Author contributions

GX: Conceptualization, Data curation, Formal Analysis, Methodology, Writing–original draft, Writing–review and editing. XH: Conceptualization, Data curation, Investigation, Software, Supervision, Writing–original draft. ZX: Conceptualization, Methodology, Validation, Visualization, Writing–review and editing. GS: Conceptualization, Formal Analysis, Funding acquisition, Investigation, Writing–review and editing. XH: Conceptualization, Writing–review and editing. ZN: Investigation, Writing–review and editing. LQ: Software, Writing–review and editing. YY: Software, Writing–review and editing.

Funding

The author(s) declare that financial support was received for the research, authorship, and/or publication of this article. This work was supported by Technology Projects of State Grid Corporation of China (5500-202318115A-1-1-ZN).

Conflict of interest

Authors ZN and LQ were employed by State Grid Jiangsu Electric Power Co., Ltd. Research Institute.

The remaining authors declare that the research was conducted in the absence of any commercial or financial relationships that could be construed as a potential conflict of interest.

The authors declare that this study received funding from State Grid Corporation of China. The funder had the following involvement in the study: interpretation of data.

Generative AI statement

The author(s) declare that no Generative AI was used in the creation of this manuscript.

Publisher's note

All claims expressed in this article are solely those of the authors and do not necessarily represent those of their affiliated

organizations, or those of the publisher, the editors and the reviewers. Any product that may be evaluated in this article, or claim that may be made by its manufacturer, is not guaranteed or endorsed by the publisher.

References

- Chowdhury, M.M.-U.-T., Biswas, B. D., and Kamalasan, S. (2023). Second-order cone programming (SOCP) model for three phase optimal power flow (OPF) in active distribution networks. *IEEE Trans. Smart Grid* 14 (5), 3732–3743. doi:10.1109/TSG.2023.3241216
- Cong, P., Tang, W., Lou, C., Zhang, B., and Zhang, L. (2019). Two-stage coordination optimization control of soft open point and tie switch in active distribution network with high penetration renewable energy generation. *Trans. China Electrotech. Soc.* 34 (06), 1263–1272. doi:10.19595/j.cnki.1000-6753.tces.180324
- Gan, G., Wang, Z., Zhou, Y., Li, L., and Li, X. (2015). Reliability and economy based closed-loop operation modes for medium voltage distribution networks. *Automation Electr. Power Syst.* 39 (16), 144–150. doi:10.7500/AEPS20140901004
- Hu, X., Liu, Z., Wen, G., Yu, X., and Liu, C. (2020). Voltage control for distribution networks via coordinated regulation of active and reactive power of DGs. *IEEE Trans. Smart Grid* 11 (5), 4017–4031. doi:10.1109/TSG.2020.2989828
- Huang, Y., Cai, Z., Pan, T., and Chen, J. (2019). Research on wide area protection and control scheme for closed-loop distribution network. *J. Electr. Power Sci. Technol.* 34 (02), 47–52. doi:10.3969/j.issn.1673-9140.2019.02.007
- Li, H., Gao, Y., Zhang, X., Lin, D., Qiang, W., and Sun, W. (2018). Promotion strategy of photovoltaic accommodation ability for regional power grid. *Electr. Power Autom. Equip.* 38, 114–120. doi:10.16081/j.issn.1006-6047.2018.07.015
- Li, J. (2019). *Robust optimal dispatching of the active distribution network with renewable energy*. Beijing: North China Electric Power University. [dissertation thesis].
- Li, Q., Zhang, N., Gao, S., Liu, J., and Zhou, Q. (2021). Modeling and application scenario analysis of power phase shift transformer based on RTDS. *Electr. Power Eng. Technol.* 40 (02), 53–58. doi:10.12158/j.2096-3203.2021.02.008
- Li, Q., Zhang, N., Gao, X., Zhao, X., and Gao, S. (2024). Bi-level optimization of distribution network reconfiguration based on new-type phase shifting transformer. *Power Demand Side Manag.* 26 (02), 14–19. doi:10.15913/j.cnki.kjycx.2024.02.006
- Li, Y., Ling, F., Qiao, X., Zhong, J., and Cao, Y. (2024). Day-ahead and intra-day optimization of flexible interconnected distribution system with self-energy storage based on the grid-side resource coordination. *Trans. China Electrotech. Soc.*, 1–17. doi:10.19595/j.cnki.1000-6753.tces.221929
- Liu, Y., Wu, W., Zhang, B., and Li, Z. (2014). A mixed integer second-order cone programming based active and reactive power coordinated multi-period optimization for active distribution network. *Proc. CSEE* 34, 2575–2583. doi:10.13334/j.0258-8013.pcsee.2014.16.007
- Samadi, P., Mohsenian-Rad, H., Wong, V. W. S., and Schober, R. (2014). Real-time pricing for demand response based on stochastic approximation. *IEEE Trans. Smart Grid* 5 (2), 789–798. doi:10.1109/TSG.2013.2293131
- Shen, X., Zhu, S., and Zheng, J. (2015). Active distribution network planning-operation co-optimization considering the coordination of ESS and DG. *Power Syst. Technol.* 39 (07), 1913. doi:10.13335/j.1000-3673.pst.2015.07.023
- Wang, C., Fang, R., Lei, H., Sun, J., and Zha, X. (2024). Day-ahead and intraday coordinated economy schedule method based on the optimal operation region in the active distribution network. *Power Syst. Technol.*, 1–16. doi:10.13335/j.1000-3673.pst.2023.0537
- Wang, Y., and Liu, X. (2022). Day-ahead and intra-day two-stage optimal control of photovoltaic-energy storage charging station based on GRU-MPC. *Electr. Power Autom. Equip.* 42 (10), 177–183. doi:10.16081/j.epae.202208036
- Wu, Z., Peng, X., Shen, Y., Xu, L., Wu, J., Lin, C., et al. (2013). Study on a loop power supply model and its loop-close operation mode for distribution network. *Proc. CSEE* 33 (10), 57–63. doi:10.13334/j.0258-8013.pcsee.2013.10.008
- Xiong, Z., Chen, T., Du, L., Dai, Z., Chen, J., and Xu, L. (2021). Optimal allocation of soft open point in active distribution network based on improved sensitivity analysis. *Automation Electr. Power Syst.* 45 (08), 129–137. doi:10.7500/AEPS20191021004
- Xu, B., Zhao, J., Zhang, P., Fan, S., and He, G. (2023). High-proportion renewable energy accommodation method based on customer directrix load and nash bargaining. *Automation Electr. Power Syst.* 47 (15), 36–45. doi:10.7500/AEPS20221130016
- Xu, L., Zhang, S., Ye, L., Cao, Y., and Cheng, H. (2024). Joint planning of source-network-load-storage in distribution network considering dynamic reconfiguration and intelligent soft open point. *South. Power Syst. Technol.*, 1–11. doi:10.13648/j.cnki.issn1674-0629.2024.04.014
- Xu, Z., Liu, J., Jiang, Y., Xi, X., and Yang, S. (2023). Loop closing control device and control method of 10 kV distribution network based on phase shifting transformer and voltage regulating transformer. *South. Power Syst. Technol.* 17 (03), 85–96. doi:10.13648/j.cnki.issn1674-0629.2023.03.010
- Xu, Z., Tang, J., Jiang, Y., Qin, R., Ma, H., Yang, Y., et al. (2022). Analysis of fault characteristics of distribution network with PST loop closing device under small current grounding system. *Energies* 15, 2307. doi:10.3390/en15072307
- Xue, R. (2020). *Location method for single phase-to-ground fault in closed-loop medium voltage distribution network*. Beijing: North China Electric Power University. [dissertation thesis].
- Yang, L. (2022). *DC transformation of contact line and operation strategy in high permeability photovoltaic distribution network*. Jiangsu: Southeast University. [dissertation thesis].
- Yang, Y., Tang, J., Niu, C., Xu, Z., and Zhao, C. (2022). Coupling characteristic and control strategy for loop closing device based on improved phase shifting transformer under three-phase asymmetry condition. *Automation Electr. Power Syst.* 46 (14), 158–168. doi:10.7500/AEPS20211216006
- Zeng, B., and Zhao, L. (2013). Solving two-stage robust optimization problems using a column-and-constraint generation method. *Operations Res. Lett.* 41 (5), 457–461. doi:10.1016/j.orl.2013.05.003
- Zheng, H., and Shi, T. (2019). Bi-level optimization of distribution network based on soft open point and reactive power compensation device. *Automation Electr. Power Syst.* 43 (19), 117–123. doi:10.7500/AEPS20180913008